이학석사 학위논문

The effect of Human Umbilical Cord Blood-derived Mesenchymal Stem Cells in Collagenase induced Intracerebral Hemorrhage Rat model

콜라겐 분해효소 유도 대뇌출혈 쥐 모델에서 인간 제대혈 유래 중간엽 줄기세포의 효과 연구

2014년 8월

서울대학교 대학원

협동과정 뇌과학과

김 관 우

A Thesis for the Degree of Master

콜라겐 분해효소 유도 대뇌출혈 쥐 모델에서 인간 제대혈 유래 중간엽 줄기세포의 효과 연구

The effect of Human Umbilical Cord Blood-derived Mesenchymal Stem Cells in Collagenase induced Intracerebral Hemorrhage Rat model

Autust 2014

Interdisciplinary Program in Neuroscience
Seoul National University
Kwan-Woo Kim

The effect of Human Umbilical Cord Blood-derived Mesenchymal Stem Cells in Collagenase induced Intracerebral Hemorrhage Rat model

지도교수 백 선 하

이 논문을 협동과정 뇌과학 석사학위논문으로 제출함

2014년 6월

서울대학교 대학원

협동과정 뇌과학 전공

김 관 우

김관우의 석사학위논문을 인준함

2014년 6월

위 원 장 이 광 우 (인)

부위원장 백 선 하 (인)

위 원 이 승 훈 (인)

The effect of Human Umbilical Cord Blood-derived Mesenchymal Stem Cells in Collagenase induced Intracerebral Hemorrhage Rat model

By

Kwan-Woo Kim

A Thesis Submitted to the Department of Natural Science in Partial Fulfillment of the Requirements for the Degree of Master in Interdisciplinary Program in Neuroscience at Seoul National University

June 2014

Approved by thesis committee:

Professor _____ Chairman

Professor _____ Vice Chairman

Professor _____ Member

Abstract

Purpose: Intracerebral hemorrhage (ICH) is one of the devastating types of stroke and has a high risk of morbidity and mortality. Human umbilical cord blood-derived mesenchymal stem cells (hUCB-MSCs) have potential to help the brain damage recovered following ICH. The purpose of this study is to identify beneficial effects of the transplantation of hUCB-MSCs in the ICH rat model and investigate whether hUCB-MSCs may have the ani-inflammatory properties by neurotrophic factors or cytokines for ICH brain.

Material & Method: hUCB-MSCs were transplanted in collagenase induced ICH rat model. At 2, 9, 16, 30 days after ICH, rotarod test and limb placement test were performed to measure behavioral outcomes. ICH rats were sacrificed to evaluate volume of lesion using H&E staining. Neurogenesis, angiogenesis, anti-apoptosis in the brain tissue of the rats was examined by immunofluorescence staining at 4 weeks after transplantation. Anti-inflammatory factors [TNF-α, COX-2, microglia and neutrophil were analyzed by immunofluorescence staining, RT-PCR and Western blot at 3 days after

transplantation.

Results: hUCB-MSCs transplantation after ICH was associated with the effect of neurological benefits and reducing volume of lesion. hUBC-MSCs treated group revealed high level of neurogenesis, angiogenesis and anti-apoptosis at 4 weeks after transplantation. The expression of inflammatory factors were decreased in rats of hUCB-MSCs treated group compared with rats of control group.

Conclusion: Our study suggests that hUCB-MSCs may improve neurological outcome and modulate inflammation-associated immune cells and cytokines in ICH-induced inflammatory responses.

Keywords: Intracerebral hemorrhage. Human umbilical cord blood-derived mesenchymal stem cells, inflammation, cytokine.

Student Number: 2010-20394

Contents

List of figures

List of table

List of Abbreviation

ICH	intracerebral hemorrhage
hUCB-MSCs	human umbilical cord blood-derived mesenchymal stem cells
TNF-α	tumor necrosis factor-alpha
COX-2	cyclooxygenase-2
RT-PCR	reverse transcription polymerase chain reaction
ESCs	embryonic stem cells
NSCs	neural stem cells
MCAO	middle cerebral artery occlusion
MNCs	mononuclear cells
α-MEM	alpha-minimum essential medium
FBS	fetal bovine serum
EDTA	ethylenediaminetetraacetic acid
i.m.	intramuscular
PBS	phosphate-buffered saline
OCT	optimal cutting temperature
H&E	hematoxylin and eosin
HuNu	human nuclei
Tuj-1	neuron specific beta Ⅲ tubulin
CD11b	integrin alpha M chain, microglia marker

MPO	myeloperoxidase, enzyme expressed in neutrophil
IgG	immunoglobulin G
TUNEL	terminal deoxynucleotidyl transferase dUTP nick end labeling
DAPI	4’,6-diamidino-2-phenylindole
GAPDH	glyceraldehyde-3- phosphate dehydrogenase
BCA	bicinchoninic acid
SDS	sodium dodecyl sulfate
PVDF	polyvinylidene fluoride
NFDM	non-fat dried milk
SVZ	subventricular zone
ANOVA	analysis of variance
DAMPs	danger-associated molecular patterns
CNS	central nervous system
MIF	macrophage/microglial inhibitory factor
TGF-β1	transforming growth factor-beta 1
HGF	hepatocyte growth factor
SDF-1	stromal cell-derived factor 1
OA	osteoarthritis
BDNF	brain-derived neuroptophic factor
CNTF	ciliary neurotrophic factor
ICAM-5	intracellular adhesion molecule-5
IL-1 ra	interleukin-1 receptor antagonist

M-CSF	macrophage colony-stimulating factor
OSM	oncostatin M
SAH	subarachnoid hemorrhage

Ⅰ. Introduction

Intracerebral hemorrhage (ICH) is one of the devastating types of stroke and has a high risk mortality and morbidity accounting for about 40% at 1 month [1]. The blood clot (hematoma) is common cause of ICH, the hematoma induced ICH increases intracranial pressure, causes of edema formation, neuronal death, and brain atrophy [2]. Management of ICH may include medical and surgical treatments to stop the bleeding, remove the clot, and reduce the pressure on the brain [3]. Despite the standard therapy and ongoing clinical trials to improve outcome in ICH, the prognosis is generally poor after ICH and the patients who survive have neurological deterioration [4].

Recent studies have investigated experimentally the therapeutic effect of stem cells [5]. Stem cells are undifferentiated progenitor cells that have the ability to proliferate and produce many different types of cell line. In several studies using stem cells, the therapeutic effects of stem cells transplantation was observed in experimental ICH animal models [6]. Of the stem cells that may be useful in ICH; embryonic stem cells (ESCs), neural stem cells (NSCs), mesenchymal stem cells (MSCs), human umbilical cord blood-

derived mesenchymal stem cells (hUCB-MSCs) have been regarded an ideal source. Besides having self-renewal ability and they differentiate into multiple lineages, MSCs isolated from umbilical cord blood have relatively few ethical concerns, low immune rejection response and tumor formation [7].

It was reported that transplantation of MSCs are able to improve recovery the brain damage following ICH. ICH rat model, MSCs promoted neurogenesis, functional recovery and reduced hemorrhage volume and apoptosis [8]. In addition, MSCs could promote angiogenesis and inhibit inflammation [9]. Particularly, recent studies revealed that inflammation has an important role in brain recovery after ICH as well as in damage of brain [10]. Furthermore, MSCs may modulate inflammation-associated immune cells and cytokines in cerebral inflammatory response [11]. However, the underlying mechanisms of hUCB-MSCs with inflammation remain largely unknown.

Previous studies, we observed that hUCB-MSCs have therapeutic effect in rat ischemia models induced by MCAO. In this study, we examined the transplantation of hUCB-MSCs in the ICH rat model have beneficial effects for neuropathological and behavioral deficit. Then, we investigated whether hUCB-MSCs may have the anti-inflammatory properties by neurotrophic factors or cytokines for ICH brain.

Ⅱ. Materials & Methods

Preparation of hUCB-MSCs

MSCs from hUCB were provided by MEDIPOST Co., Ltd. (Seoul, Korea). This study was approved by the Institutional Review Board of the Seoul National University Hospital and the Institutional Review Board of MEDIPOST Co., Ltd. Umbilical cord blood was collected from umbilical veins after neonatal delivery with informed consent of the pregnant mother. MSCs were isolated from mononuclear cells (MNCs) using a Ficoll-Hypaque solution (d = 1.077 g/ cm^3; Sigma). Following transfer to α-minimum essential medium (α-MEM; Gibco) supplemented with fetal bovine serum (FBS; Gibco), MSCs were seeded in culture flasks at 5 x 10^5 cells/cm^2. Cells maintained in humidified 5% CO_2 at 37℃ formed colonies of spindle- shaped cells. At 50% confluence, cells were harvested after treatment with 0.25% (w/v) trypsin- EDTA (Gibco) and were reseeded for expansion.

Animal procedures

Adult male Sprague-Dawley rats (250-300 g; Orient, Gapyeong, Korea) were housed in the same animal care facility

under a 12 hours light/dark cycle with food and water ad libitum. Animal care and surgical procedures were performed in accordance with guidelines approved by the Experimental Animals Committee of Seoul National University Hospital for the ethical use of animals. All efforts were made to minimize suffering and number of animals used in experiments.

Collagenase induced ICH model

Rats were anesthetized using an intramuscular (i.m.) injection of 1% zoletil (20 mg/kg) and xylazine hydrochloride (5 mg/kg). Rectal temperature was maintained at 37℃ via a thermistor-controlled heating blanket (Panlab, Heidelberg, Germany) throughout the surgery. Animals were placed in a stereotaxic apparatus to induce ICH by collagenase. In brief, 1 μl (0.2 μl/min) of saline containing 0.2 units of bacterial collagenase (type VII; Sigma) was injected stereotaxically into the striatum at coordinates 3.0 mm lateral to bregma and 5.0 mm ventral to the cortical surface. After injection, the Hamilton syringe was left in place for 5 minutes. The needle was slowly removed after an additional 10 minutes delay to prevent backflow. The hole was sealed with bone wax and the wound was sutured.

Transplantation of hUCB-MSCs

Two days after injection of collagenase into striatum, we performed behavioral tests and randomly divided rats into 2 groups: rats of control group were injected with 5 μl of 10 x PBS; experimental group, transplantation of 5 x 10^5 MSCs in 5 μl of PBS were injected stereotactically into the left lateral ventricle of anesthetized animals at 3.0 mm lateral to bregma and 5.0 mm ventral to the cortical surface. Animals were not given any prophylactic immunosuppressant.

Behavioral test

In all animals, behavioral tests were performed on 1 day before ICH and at 2, 9, 16, 30 days after ICH as shown in Figure 1. Motor behavioral performance was evaluated by an accelerating Rotarod apparatus and a modified version of the limb placement test described by De Ryck which has been widely used for functional scoring in stroke models.

The rotarod test was performed to evaluate the degree of coordinated movements. All rats were trained at a constant speed of 16 rpm (600 seconds) for 3 days before ICH. The mean duration (in seconds) on the device was recorded for three rotarod test measurements 1 day before surgery. The rats are placed on the accelerating rod (speed from 3.5 to 35 rpm) and the time, the rats remained on the rotarod was

measured three times. Rotarod test data are presented as percentile of the maximal duration compared with the baseline control (before ICH).

The limb placement test has three limb-placing tasks that assess the motor integration of forelimb and hindlimb responses to tactile and proprioceptive stimulations. The test consists of three domains: (1) visual forward, (2) visual lateral, and (3) proprioception. The tasks were scored in the following manner: the 'visual forward' is observation of forelimb flexion by holding up the tail. The stretch of the forelimbs towards the table is evaluated: normal stretch, 0 point; abnormal flexion, 1 point. The 'visual lateral' is observation of forelimb stretch by the stimulus to rat's whiskers while the examiner holds the rat's trunk. The visual lateral makes a score 0, 1, 2 and 3 points: normal lifting, 0 point; abnormal lifting, 1, 2, 3 points according to the times of normal stretch. The 'proprioception' is observation of stepping up of forelimb and hindlimb on the table after pulling down the forelimb and hindlimb below the level of the table in three times each: normal lifting, 0 point; abnormal lifting, 1, 2, 3 points according to the times of normal stretch. The authors defined the severity of injury by the score graded on a scale of 0 to 10 (normal score 0, maximal deficit score 10).

Histological examination

When behavior tests were finished at 30 days after ICH, the animals were anesthetized and intracardiac perfusion with saline followed by ice-cold 4% paraformaldehyde in PBS (pH 7.4) was performed for 10 min. Brains were removed, post-fixed for one day at 4℃, and then cryoprotected overnight in the same fixative supplemented with 25% sucrose. The tissues were embedded in OCT compound (Sakura Finetek, Inc., Torrance, CA), and frozen at −70℃ with dry ice. Coronal sections (14 ㎛ thick; 28 ㎛ apart) were taken with a cryostat (Leica Microsystems, Wetzlar, Germany). Sections were stained with Hematoxylin and Eosin (H&E), and the volume of lesion (e.g., cavity, cellular debris) was calculated using ImageJ 1.38x (National Institutes of Health, Wayne Rasband, USA)

$$\text{volume of lesion}(mm^3) = \text{area of lesion } (mm^2) \times \text{thickness of slice (mm/slice)} \times \text{sampling interval (slice)}$$

Immunofluorescence staining

The sections were washed with 1X PBS, permeabilized with PBS containing 0.1% (v/v) saponin and 4% (v/v) normal goat

serum (NGS) for 30 min at 25 and blocked with PBS containing 0.05% (v/v) saponin and 5% (v/v) NGS for 30 min. The sections were also permeabilized for 30 min with 0.1% (v/v) Triton X. The sections were incubated overnight at 4 ℃ with primary antibody. Subsequently, sections were incubated for 1hr at room temperature with a fluorescence labeled secondary antibody and mounted with Vectashield medium containing DAPI (Vector Laboratories, Burlingame, CA). The primary antibodies used in experiments included mouse anti-Human Nuclei (1:100; MAB4383, Chemicon, CA), rabbit anti-laminin (1:200; L9393, Sigma, Inc., MO), rabbit anti-neuron specific beta Ⅲ tubulin (Tuj-1)(1:100; ab18207, abcam, UK), rabbit anti-COX2 (1:100; ab15191, abcam, UK), mouse anti-TNF alpha (1:100; ab1793, abcam, UK), mouse anti-CD11b (1:100; BD Pharmingen, CA), and rabbit anti-myeloperoxidase (1:100; ab45977, abcam, UK) All secondary antibodies, Alexa 488, Alexa 594 goat anti-mouse IgG, and goat anti-rabbit IgG, were purchased from Molecular Probes (Invitrogen, Co., CA). The In Situ Cell Death Detection Kit, TMR red (Roche) was used for indirect TUNEL staining.

Fluorescently immunolabeled sections were imaged by confocal laser scanning microscope (model Leica TCS SP8; Leica Microsystems, Inc., Mannheim, Germany) equipped with many

lasers (Diode 405, Argon 488, DPSS 561, HeNe 594 and HeNe 633). Each channel was separately scanned using a sequential scan for confocal imaging without bleed-through between channels. To visualize whole brain image, Tile scanning was performed at a magnification of 10x (PL APO 0.40), 20x (PL APO 0.70) and then the tile scan images ware merged. To evaluate a labeling, confocal scanning was performed at a magnification of 40x (PL APO 1.1 W). Images were acquired using the LAS AF software. Staining density was analyzed using Image-Pro Plus 4 (Media Cybernetics, Bethesda, MD).

RT-PCR (reverse transcription-polymerase chain reaction)

RNA was isolated at day 5 after ICH using RNeasy Lipid Tissue Mini Kit (QIAGEN, Hilden, Germany). First-strand cDNA synthesis was carried out by random priming of the total RNA using a random primer mixture (Invitrogen) and reverse transcriptase with superscript 3 (Invitrogen). The sequences of the primers and the cycles of PCR are given in Table 1. The PCR products were resolved in 1% agarose gels. The band density from gel images was determined by Gel Doc XR System (BIO-RAD, Segrate, Italy). The sequences of the primers and

the cycles of PCR are given in Table 1. Rat glyceraldehyde-3-phosphate dehydrogenase (GAPDH) was used as an internal control.

Western Blot Analysis

Brain protein was isolated at 5 days after ICH. Animals were anesthetized and decapitated, and whole brains were cut in 2 mm coronal sections, and then rapidly divided into ipsilateral (infarcted) and contralateral hemispheres, which were snapped and frozen in liquid nitrogen. Brain tissues from each group were homogenized in Neuronal Protein Extraction Reagent (Pierce, Rockford, USA), which included 1X protease and phosphatase inhibitor (Pierce, Rockford, USA), followed by incubation on ice for 10 minutes. Samples were centrifuged at 10,000g at for 10 minutes at 4℃ to pellet the cell debris. Protein concentrations were determined using BCA Protein Assay Kit (Pierce, Rockford, USA) with bovine serum albumin as a standard. Aliquots (total volume 20 μl) containing 20μl total protein diluted into 5X sample buffer (Pierce, Rockford, USA) were separated by electrophoresis on 10% SDS-polyacrylamide gels. Proteins in the gels were then electrotransfered onto polyvinylidene fluoride (PVDF) membranes (Amersham, Little Chalfont, UK), which were

blocked for 1 hour in 5% non-fat dried milk (NFDM) in TBST (0.5 M Tris-HCl, pH 7.4, 1.5 M NaCl containing 0.1% Tween-20), followed by incubation overnight at 4℃ with rabbit anti-COX2 (1:1000; ab15191, abcam), mouse anti-TNF alpha (1:1000; ab1793, abcam), mouse anti CD11b (1:500; 554980, BD Pharmingen), and rabbit anti-myeloperoxidase (1: 1000; ab45977, abcam) and b-actin diluted in TBST containing 5% NFDM. Membranes were extensively washed with TBST, and then incubated for 1 hour with horseradish peroxidase-conjugated goat anti-mouse IgG (Vector) or anti- rabbit IgG (Vector) diluted 1:3000 in TBST. Proteins were visualized using SuperSignal West Femto Maximum Sensitivity Substrate (Pierce, Rockford, USA). The intensity of all protein bands was quantified by densitometry using the Bio-image Processing System (GenDix, Seoul, Korea). Densitometric values were normalized to those of beta-actin, used as an internal control.

Statistical analysis

Data are presented as mean±SEM. The significance of differences between test conditions was assessed using Mann-Whitney U test. Comparisons of continuous variables between two groups were performed by a two-way ANOVA. $p<0.05$ was considered statistically significant. The GraphPad Prism 5

software (GraphPad Prism, San Diego Califormia, USA) was used for the statistical tests.

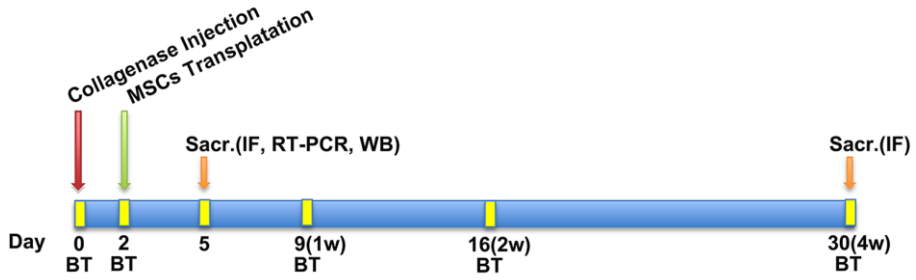

Figure 1. Timeline of the experimental procedures.

Animals were injected with collagenase at day 0. After 2 days, animals were transplanted intracerebrally with MSCs. Inflammation groups were sacrificed to perform immunofluorescence staining, RT-PCR and western blotting at day 5 after ICH and another groups were sacrificed to perform immunofluorescence staining and measure hemorrhage volume at day 30. Behavior tests were performed before injection collagenase and at 2, 9, 16, 30 days after ICH. MSCs indicates mesenchymal stem cells; Sacr, sacrifice; IF; immunofluorescence staining; WB, western blot; and BT, behavior test.

Table 1. Oligonucleotide primers used in this study for RT-PCR

Gene	Sense/antisense	Size of Product(bp)	Annealing temperature (°C)	Cycle of the PCR
TNF-a	CCCAGACCCTCACACTCAGAT	215	60	40
	TTGTCCCTTGAAGAGAACCTG			
COX2	GCTGTGCTGCTCTGCGCTTGCCCTGGC	308	58	35
	GATCTGGACGTCAACACGTATCTCATG			
CD11b	GCCTGATGGACTTGGCTGT	322	60	40
	ACCCGGATGCGCCTGAGTAT			
MPO	GCCATGGTCCAGATCATCAC	283	65	40
	TGGGGTCAATGCCACCTTCC			
GAPDH	AAGGTCATCCCAGAGCTGAA	338	57	21
	ATGTAGGCCATGAGGTCCAC			

Ⅲ. Result

Volume of lesion in transplanted hUCB-MSCs

Hemorrhagic lesions mainly appeared in the striatum by hematoxylin and eosin staining at 30 days after ICH. Ventricles were observed more expanded in ipsilateral hemisphere than contralateral hemisphere (Fig. 2a). The volume of lesion in the rats injected with the hUCB-MSCs were significantly smaller than those of the rats injected with PBS at 4 weeks after transplantation (Fig. 2b, $p<0.01$). These results indicate that hUCB-MSCs reduce the volume of lesion in rats after ICH.

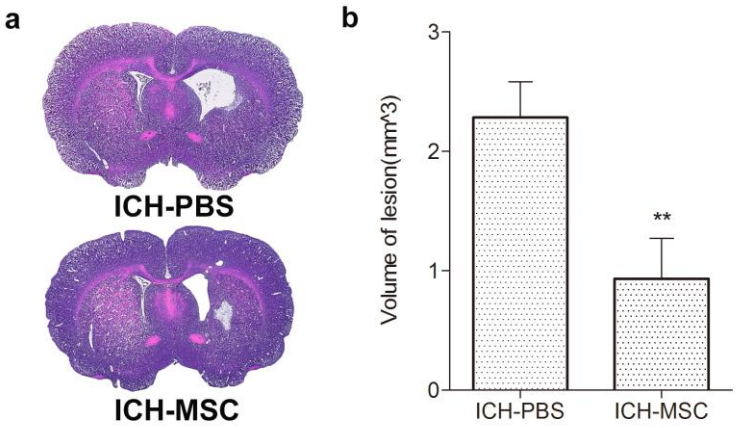

Figure 2. Volume of lesion following the transplantation of hUCB-MSCs into ICH rats.

ICH rats treated with hUCB-MSCs were compared to ICH rats. (a) H&E staining of coronal sections for characterization of the unilateral brain injury at 30 days after ICH. (b) The volume of lesion in hUCB-MSCs transplanted group (n=8) were significantly smaller than PBS control group (n=10) at 4 weeks after transplantation. ** $p<0.01$. The volume of lesion was determined by summation of the lesion area and measured analysis of Mann-Whitney U test. Data is shown as mean and SEM.

Neurological function in transplanted hUCB-MSCs

ICH involves behavioral deficit. To evaluate behavioral outcome, rotarod test and limb placement test were performed (Fig. 1). ICH rats receiving hUCB-MSCs (n=8) were able to remain on the rotarod for significantly longer time than animals receiving PBS (n=10) at 4 weeks after transplantation (Fig. 3a, $p<0.001$). The effect was also observed in Limb placement test. At 4 weeks after hUCB-MSCs treatment, the Limb test score revealed significant neurological benefit in the ICH group transplanted hUCB-MSCs as compared with the PBS treated group (Fig. 3b, $p<0.01$). These results indicate that hUCB-MSCs promotes functional recovery in rats after ICH.

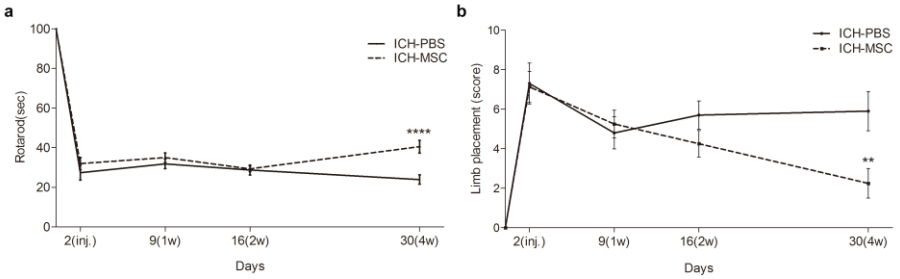

Figure 3. Result of behavioral improvement following the transplantation of hUCB-MSCs into ICH rats.

Behavioral improvement shown in ICH rats transplanted with hUCB-MSCs. (**a**) Rotarod test. hUCB-MSCs transplanted group (n=8) showed significantly better performance than PBS control group (n=10) at 4 weeks after transplantation.; ****p<0.0001, repeated-measured analysis of variance (ANOVA). (**b**) Limb placement test. hUCB-MSCs transplanted group (n=8) showed better performance than PBS control group (n=10) at 4 weeks after transplantation.; **p<0.01, repeated-measured ANOVA. All data are shown as mean and SEM.

Endogenous neurogenesis in transplanted hUCB-MSCs

To confirm the existence of hUCB-MSCs after the transplantation into the brain, we performed immunofluorescence staining with anti-human nuclei antibody (HuNu). However, HuNu-positive cells were not detected in both experimental and control rats at 4 weeks after transplantation (data not shown).

Next we examined the endogenous neurogenesis by assessing the expression levels of Tuj1(beta Ⅲ tubulin). We used the tile scan confocal microscope image at low magnification (Fig. 4a, f; x100) and high magnification (Fig. 4b, g; x200) to find the location of expressed fluorescence. We found Tuj1-positive cells (green) in the SVZ or in the hemorrhage area at 4 weeks after tnsplantation (Fig. 4a, b, f, g). Tuj1-positive cells were increased in rats receiving hUCB-MSCs (n=8) compared with PBS control (n=10) at 4 weeks after transplantation (Fig. 4c-e, h-j; magnification x400). Statistical analysis indicated that staining for Tuj1 marker in the treated with hUCB-MSCs group had been increased compared with Control. However, there was no significant difference between the PBS- and hUCB-MSCs-treated groups (Fig. 4k).

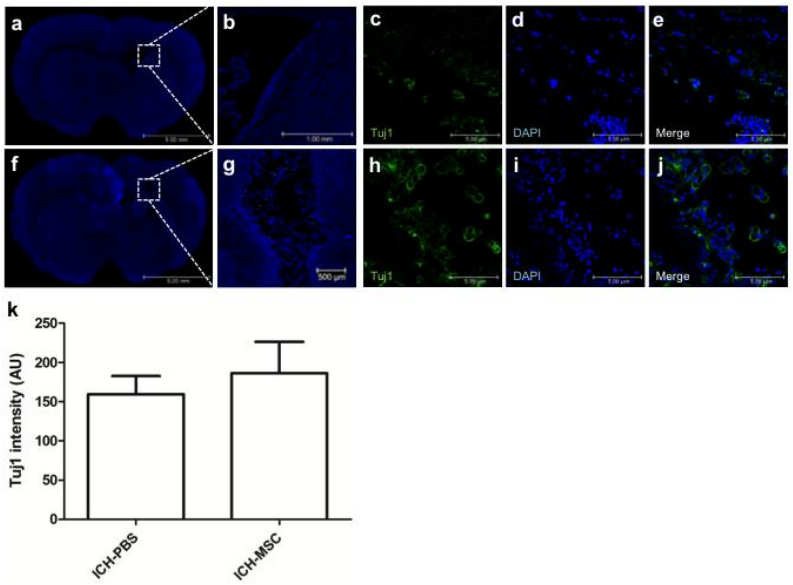

Figure 4. Representative expression of NSC specific marker following the transplantation of hUCB-MSCs into ICH rats.

(**a-j**) The rats at 4 weeks after transplantation were analyzed for presence of Tuj1 using immunofluorescence staining. (**a**, **f**) Low-magnification (x100) tile scan confocal microscopy images covering whole brain. (**b**, **g**) High-magnification (x200) tile scan confocal microscopy images covering lesion sites. Tuj1-positive cells (green) were detected in SVZ. Nuclei were counterstained with DAPI (blue). (**k**) Tuj1-positive cells were increased in rats receiving hUCB-MSCs (n=8) compared with PBS control (n=10), but there is not significant difference between PBS and hUCB-MSCs. (**c-e**, **h-j**, magnification x 400)

Angiogenesis in transplanted hUCB-MSCs

To understand whether hUCB-MSCs transplantation might have an impact on angiogenesis in the post-hemorrhagic brain, antibody for laminin was used to detect the major basement membrane of the blood vessel. We used the tile scan confocal microscope image at low magnification (Fig. 5a, f; x100) and high magnification (Fig. 5b, g; x200) to find the location of expressed fluorescence. Laminin-positive cells (green) were observed at the hemorrhage site in hUCB-MSCs treated rats and PBS-treated rats after 4 weeks after transplantation (Fig. 5a, f). Laminin-positive cells were expressed strongly in peri-infarct regions (Fig 5b, g). Laminin-positive cells were increased in rats receiving hUCB-MSCs (n=8) compared with PBS control (n=10) at 4 weeks after transplantation (Fig. 5c-e, h-j; magnification x400). Statistical analysis indicated that the number of laminin-positive cells was significantly higher in hUCB-MSCs treated rats than in PBS-treated rats after 4 weeks after transplantation (Fig. 5k, p <0.05). These results indicate that hUCB-MSCs promote angiogenesis in rats after ICH.

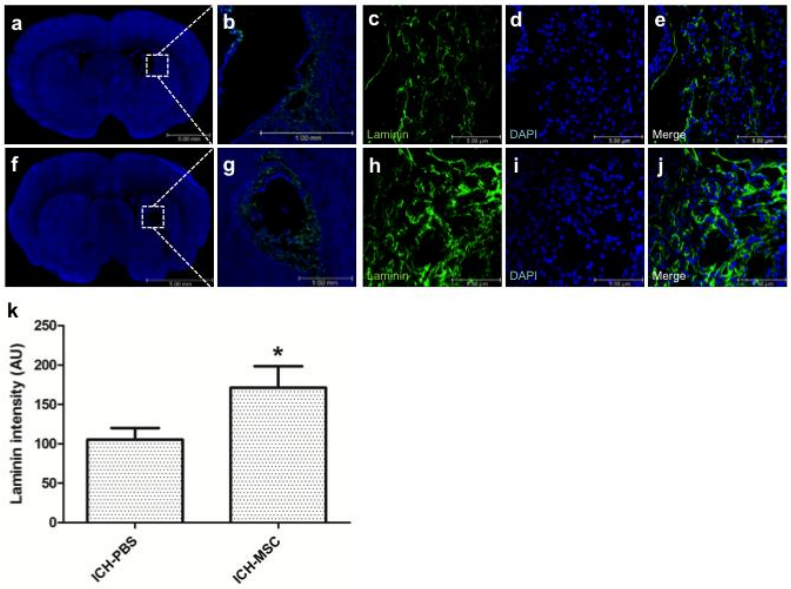

Figure 5. Representative expression of blood vessel marker following the transplantation of hUCB-MSCs into ICH rats.

(**a-j**) The rats at 4 weeks after transplantation were analyzed for presence of Laminin using immunofluorescence staining. (**a**, **f**) Low-magnification (x100) tile scan confocal microscopy images covering whole brain. (**b**, **g**) High-magnification (x200) tile scan confocal microscopy images covering lesion sites. Laminin-positive cells (green) were expressed strongly in peri-infarct regions. Nuclei were counterstained with DAPI (blue). (**k**) Laminin-positive cells were significantly increased in rats receiving hUCB-MSCs (n=8) compared with PBS treated rats (n=10). Values are shown as mean and SEM. *p <0.05 compared with the control group. (**c-e**, **h-j**, magnification x 400)

Anti-apoptosis in transplanted hUCB-MSCs

To determine if transplanted hUCB-MSCs reduce apoptosis in the ICH rat brain, we used TUNEL staining to identify apoptotic cells in the brain tissue. We used the tile scan confocal microscope image at low magnification (Fig. 6a, f; x100) and high magnification (Fig. 6b, g; x200) to find the location of expressed fluorescence. TUNEL-positive cells (red) were found within the hemorrhage lesion as well as in the surrounding periphery in hUCB-MSCs treated rats and PBS-treated rats after 4 weeks after transplantation (Fig. 6a, b, f, g). TUNEL-positive cells were decreased in rats receiving hUCB-MSCs (n=8) compared with PBS control (n=10) at 4 weeks after transplantation (Fig. 6c-e, h-j; magnification x400). Although the number of TUNEL-positive cells was decreased in the ICH animals treated with hUCB-MSCs than treated with PBS, no significant difference was found between the two groups (Fig. 6k).

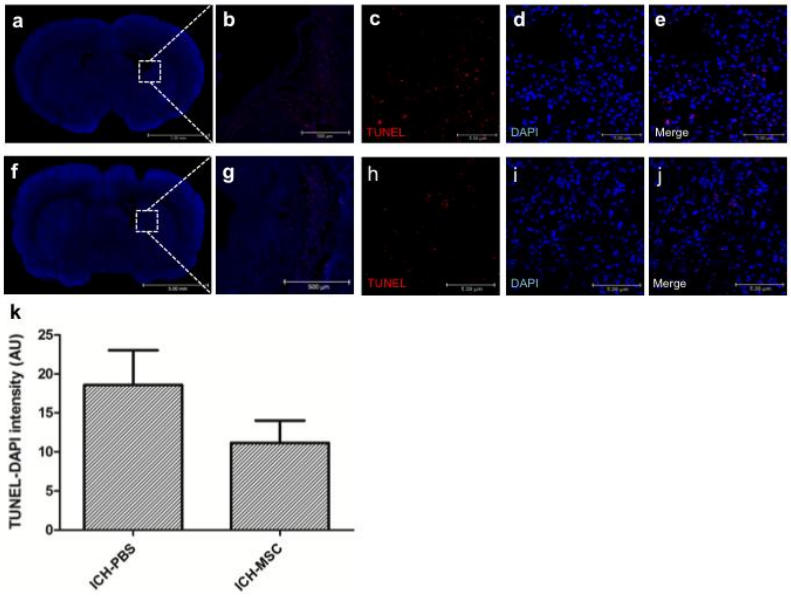

Figure 6. Representative expression of apoptotic cell marker following the transplantation of hUCB-MSCs into ICH rats.

(**a-j**) The rats at 4 weeks after transplantation were analyzed for presence of TUNEL using immunofluorescence staining. (**a**, **f**) Low-magnification (x100) tile scan confocal microscopy images covering whole brain. (**b**, **g**) High-magnification (x200) tile scan confocal microscopy images covering lesion sites. TUNEL-positive cells (red) were detected in peri-infarct regions. Nuclei were counterstained with DAPI (blue). (**k**) TUNEL-positive cells were decresed in hUCB-MSCs treated group (n=8) compared with PBS control (n=10), but there is not significant difference between PBS and hUCB-MSCs. (**c-e**, **h-j**, magnification x 400)

Anti-inflammation in transplanted hUCB-MSCs

To confirm the existence of hUCB-MSCs after the transplantation into the brain at 3 days after transplantation, we performed immunofluorescence staining with anti-human nuclei antibody (HuNu). We used the tile scan confocal microscope image at low magnification (Fig. 7a; x100) and high magnification (Fig. 7b; x200) to find the location of expressed fluorescence. HuNu-positive hUCB-MSCs (red) survived and majority of the cells were distributed close to the hemorrhagic boundary zone at 3 days after transplantation (Fig. 7a-e; c-e magnification x400).

Inflammation after ICH comprises both molecular and cellular components [12]. To investigate the effect of hUCB-MSCs in inflammation response, the inflammatory factors, tumor necrosis factor alpha (TNF)-α, Cyclooxygenase (COX)-2, CD11b-positive microglia and myeloperoxidase (MPO)-positive neutrophil were identified at 3 days after transplantation (Fig. 8-11). We used the tile scan confocal microscope image at low magnification (x100) and high magnification (x200) to find the location of expressed fluorescence.

Confocal micrographs of brain sections showed the expression of TNF-α (green) in peri-hemorrhagic regions (Fig. 8a, b, f,

g). The expression of TNF-α were decresed in hUCB-MSCs treated group (n=3) compared with PBS control (n=3) at 3 days after transplantation (Fig. 8c-e, h-j, magnification x400). However, there is not significant difference between control and hUCB-MSCs transplanted rats (Fig. 8k).

The expression of COX-2 (green) found in peri-hemorrhagic regions (Fig. 9a, b, f, g). The expression of COX-2 were decresed in hUCB-MSCs treated group (n=3) compared with PBS control (n=3) at 3 days after transplantation (Fig. 9c-e, h-j, magnification x400). However, there is not significant difference between control and hUCB-MSCs transplanted rats (Fig. 9k).

To investigate the activation of microglia, we used the antibody for CD11b expressed from activated microglia. The expression of CD11b (green) found in peri-hemorrhagic regions (Fig. 10a, b, f, g). The expression of CD11b were decresed in hUCB-MSCs treated group (n=3) compared with PBS control (n=3) at 3 days after transplantation (Fig. 10c-e, h-j, magnification x400). However, there is not significant difference between control and hUCB-MSCs transplanted rats (Fig. 10k).

To investigate the activation of neutrophils, we used the antibody for MPO expressed from activated neutrophils. the expression of MPO (green) in peri-hemorrhagic regions (Fig.

11a, b, f, g). The expression of MPO were decresed in hUCB-MSCs treated group (n=3) compared with PBS control (n=3) at 3 days after transplantation (Fig. 11c-e, h-j, magnification x400). However, there is not significant difference between control and hUCB-MSCs transplanted rats (Fig. 11k).

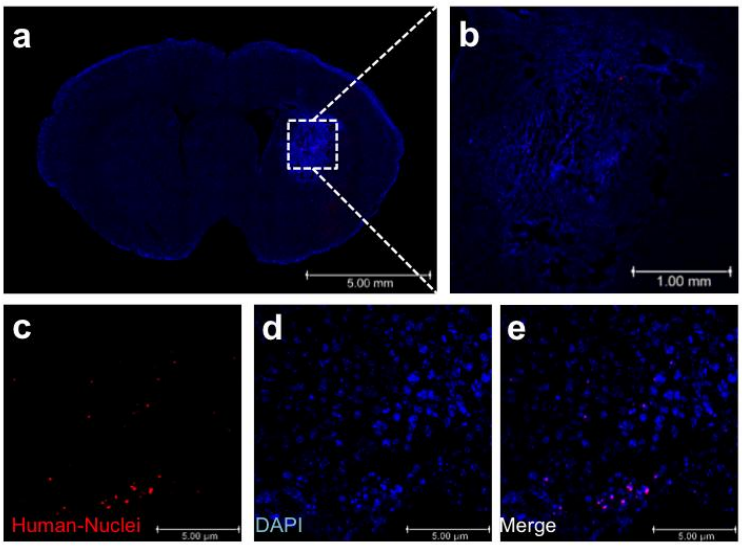

Figure 7. Representative expression of hUCB-MSCs following the transplantation of hUCB-MSCs into ICH rats.

At 3 days after 5 x 10^5 MSCs administration, hUCB-MSCs were identified by the staining with human nuclei antibody (HuNu, red) and the HuNu-positive cells in peri-infarct regions. (**a**) First figure is low-magnification (x100) tile scan confocal microscopy images covering whole brain. (**b**) Second figure is high-magnification (x200) tile scan confocal microscopy images covering lesion sites. (**c-e**) HuNu-positive cells (red) were detected in peri-infarct regions. Nuclei were counterstained with DAPI (blue). (n=3 per group). (**c-e** , magnification x400)

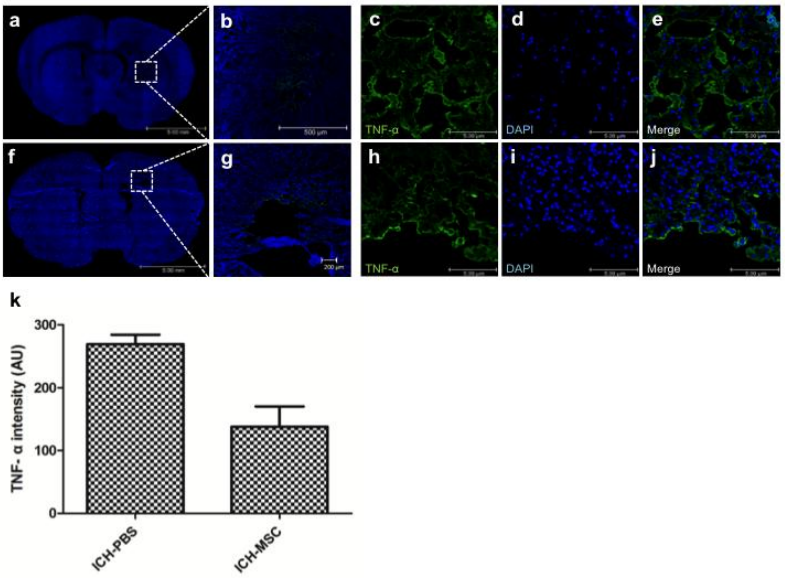

Figure 8. Representative expression of tumor necrosis factor-α following the transplantation of hUCB-MSCs into ICH rats.

The rats at 3 days after transplantation were analyzed for presence of TNF-α using immunofluorescence staining. (**a**, **f**) Low-magnification (x100) tile scan confocal microscopy images covering whole brain. (**b**, **g**) High-magnification (x200) tile scan confocal microscopy images covering lesion sites. Confocal micrographs of brain sections show the expression of TNF-α (green) in peri-hemorrhagic regions. Nuclei were counterstained with DAPI (blue). (**k**) TNF-α-positive cells were decresed in hUCB-MSCs treated group (n=3) compared with PBS control (n=3), but there is not significant difference between PBS and hUCB-MSCs. (**c-e**, **h-j**, magnification x400)

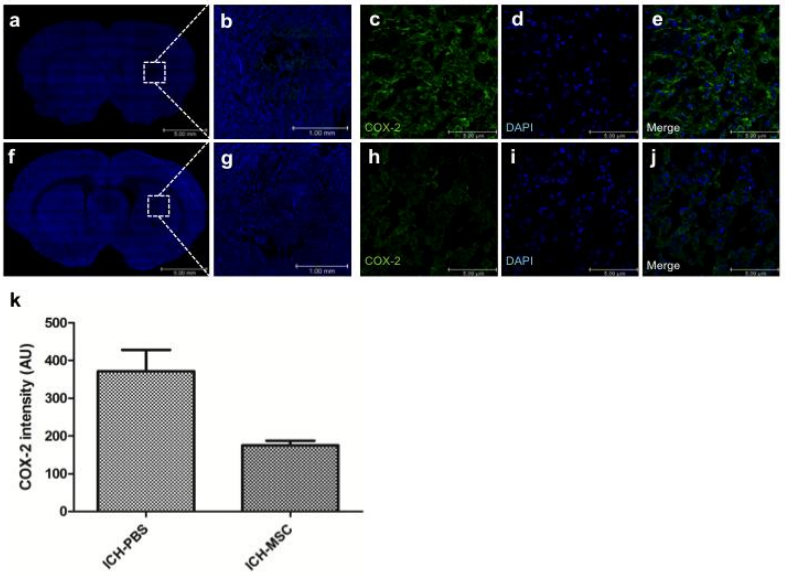

Figure 9. Representative expression of cyclooxygenase-2 following the transplantation of hUCB-MSCs into ICH rats.

The rats at 3 days after transplantation were analyzed for presence of COX-2 using immunofluorescence staining. (**a**, **f**) Low-magnification (x100) tile scan confocal microscopy images covering whole brain. (**b**, **g**) High-magnification (x200) tile scan confocal microscopy images covering lesion sites. Confocal micrographs of brain sections show the expression of COX-2 (green) in peri-hemorrhagic regions. Nuclei were counterstained with DAPI (blue). (**k**) COX-2 -positive cells were decresed in hUCB-MSCs treated group (n=3) compared with PBS control (n=3), but there is not significant difference between PBS and hUCB-MSCs. (**c-e**, **h-j**, magnification x400)

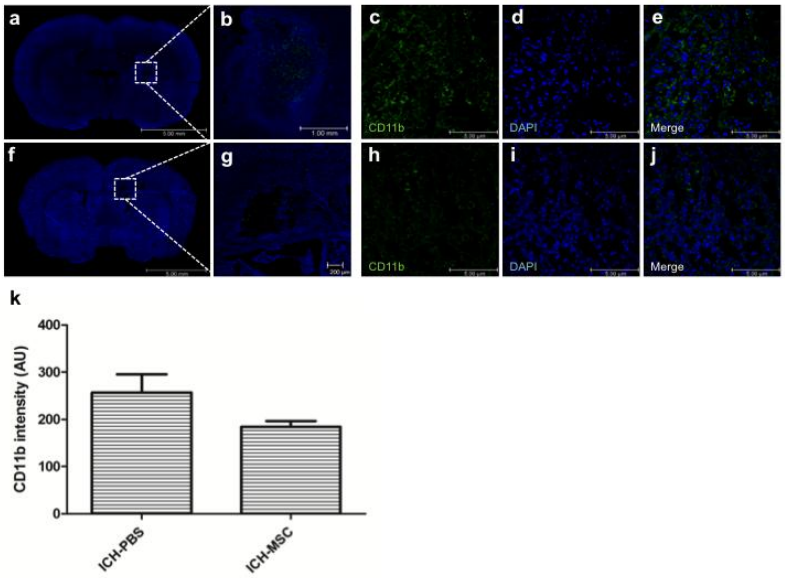

Figure 10. Representative expression of CD11b following the transplantation of hUCB-MSCs into ICH rats.

The rats at 3 days after transplantation were analyzed for presence of CD11b using immunofluorescence staining. (**a**, **f**) Low-magnification (x100) tile scan confocal microscopy images covering whole brain. (**b**, **g**) High-magnification (x200) tile scan confocal microscopy images covering lesion sites. Confocal micrographs of brain sections show the expression of CD11b (green) in peri-hemorrhagic regions. Nuclei were counterstained with DAPI (blue). (**k**) CD11b-reactive microglia were decresed in hUCB-MSCs treated group (n=3) compared with PBS control (n=3), but there is not significant difference between PBS and hUCB-MSCs. (**c-e**, **h-j**, magnification x400)

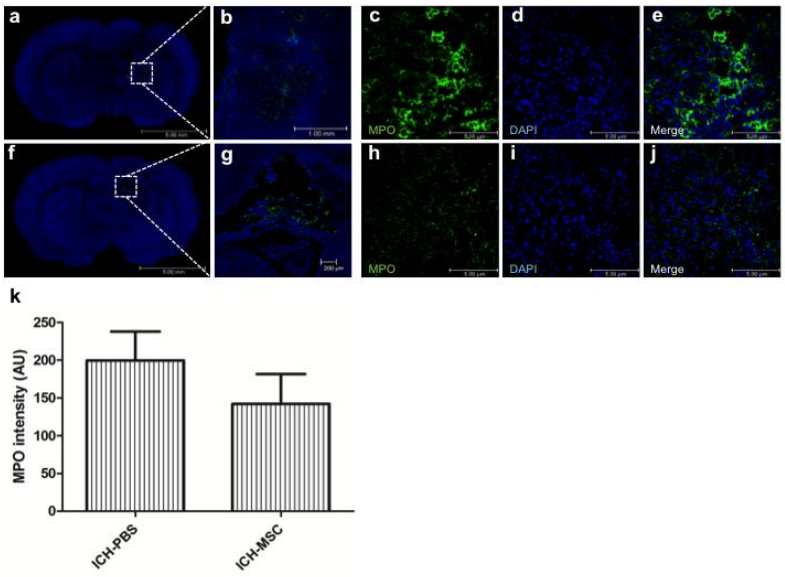

Figure 11. Representative expression of myeloperoxidase following the transplantation of hUCB-MSCs into ICH rats.

The rats at 3 days after transplantation were analyzed for presence of MPO using immunofluorescence staining. (**a**, **f**) Low-magnification (x100) tile scan confocal microscopy images covering whole brain. (**b**, **g**) High-magnification (x200) tile scan confocal microscopy images covering lesion sites. Confocal micrographs of brain sections show the expression of MPO (green) in peri-hemorrhagic regions. Nuclei were counterstained with DAPI (blue). (**k**) MPO-reactive neutrophils were decresed in hUCB-MSCs treated group (n=3) compared with PBS control (n=3), but there is not significant difference between PBS and hUCB-MSCs. (**c-e**, **h-j**, magnification x400)

mRNA and protein expression of the inflammatory factors in transplanted hUCB-MSCs

The mRNA level of TNF-α, COX-2, microglia and neutrophil, were detected by RT-PCR (Fig. 12a). The mRNA expression of these inflammatory factors were down-regulated in hUCB-MSC-treated group compared with control. However, there was not significantly difference between control and hUCB-MSCs transplanted rats (Fig. 12b-e).

The protein levels of the inflammatory factors were detected by western blot (Fig. 13a). The protein expression levels were down-regulated in the transplanted hUCB-MSC rats compared with control rats. However, there was not significantly difference between control and hUCB-MSCs transplanted group (Fig. 13b-e).

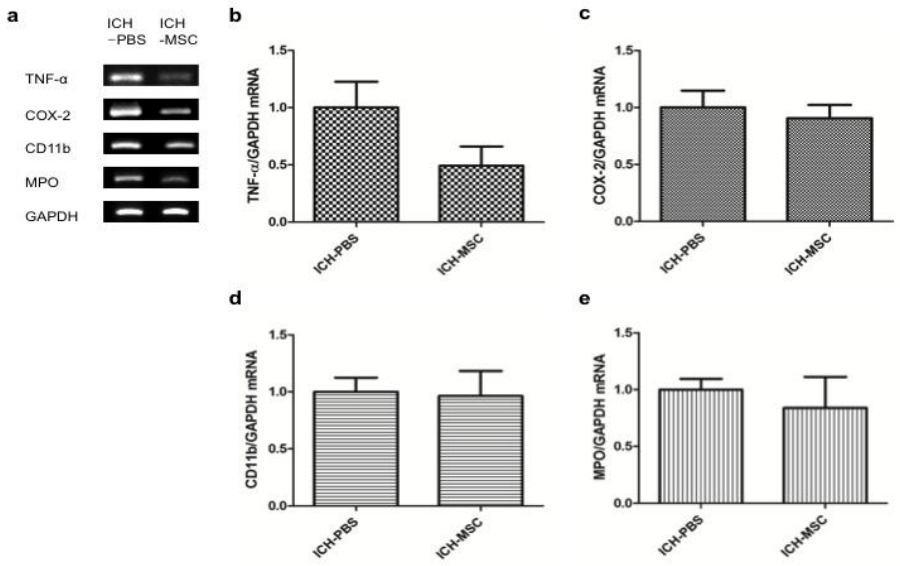

Figure 12. RT-PCR analysis of inflammatory factors mRNA expression following the transplantation of hUCB-MSCs into ICH rats.

RT-PCR products indicate specific mRNA in whole brain tissue of ICH rat at 3 days after transplantation. (a) mRNA levels of inflammatory factors including TNF-α, COX-2, CD11b and MPO. (b-e) Quantification of inflammatory factor's mRNA expression in hUCB-MSCs treated group (n=3) compared with control (n=3). Densitometric analysis was performed using Image J software with GAPDH mRNA expression as the loading control.

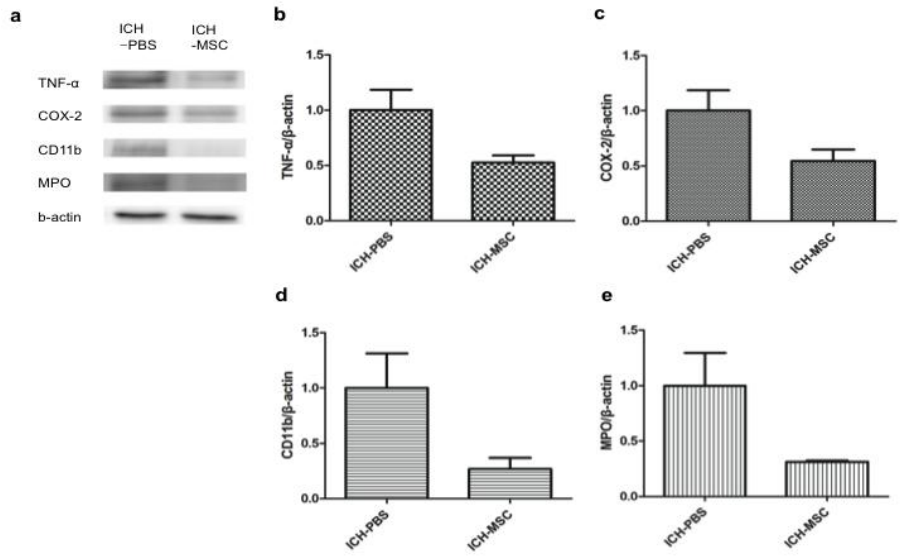

Figure 13. Western blot analysis of inflammatory factors protein expression following the transplantation of hUCB-MSCs into ICH rats.

Western blot products indicate specific protein in whole brain tissue of ICH rat at 3 days after transplantation. (a) Representative western blots of inflammatory factors including TNF-α, COX-2, CD11b and MPO. (b-e) Quantification inflammatory factor's protein expression in hUCB-MSCs treated group (n=3) compared with control (n=3). Densitometric analysis was performed using Image J software normalized to β-actin as the control.

Ⅳ. Discussion

1. Mechanism of brain injury after ICH

ICH-induced brain injury is due to physical disruption to cellular architecture of the brain and the mass of the hematoma can increase intracranial pressure, subsequently compressing brain tissue and thereby affecting blood flow and leading to brain herniation. This primary brain injury occurs at the time of hemorrhage. Secondary injury after ICH can be caused by primary injury, by the physiological response to the hematoma, and by release of clot components. This secondary brain injury can result in severe neurological deficits and death in patients with ICH [13]. Recent studies have focused on therapies focused on secondary brain injury and showed that inflammation is the key contributor of ICH-induced secondary injury. Inflammation is a normal defense response after ICH. Whoever, as ICH progresses, dead cells release danger-associated molecular patterns (DAMPs), which aggravates inflammatory injury [14]. These evidences indicate that reduction of inflammatory factors may improve neurological recovery after ICH.

2. Components of inflammatory response

Microglia are the resident innate immune cells in the central nervous system (CNS) [15]. The activation of microglia has a role in the secondary injury after ICH, although some microglia may be benefit. Microglia activation results in their production of pro-inflammatory cytokines (TNF-α, IL-1β, IL-6) and chemokines (CXCL2) [16]. In ICH animal model, the inhibition of microglial activation by tuftsin fragment 1-3 macrophage/microglial inhibitory factor (MIF) reduced the hemorrhage size and improved the neurobehavioral deficits [17]. Of the various types of leukocytes, neutrophils also infiltrates into hematoma after ICH and the infiltrating neutrophils can damage brain tissue directly by generating ROS, secreting pro-inflammatory proteases [18]. In a ICH mouse model, neutrophils depletion results in improved functional outcomes at day 3 post-hemorrhage [19].Inflammatory cytokines are classified as pro- and anti-inflammatory mediators, based on their ability to stimulate or suppress immune activation. Tumor necrosis factor-α (TNF-α), pro-inflammatory cytokine, is synthesized and released in the brain by astrocytes and some of neurons after injury [20]. In preclinical study, brain TNF-α expression is increased after ICH [21]. TNF-α antagonism by a murine infliximab improves neurological recovery after ICH [22]. COX-2 is a second and

inducible isoform of COX, rapidly expressed in several cell types in response to growth factors, cytokines, and pro-inflammatory molecules [23]. In animal models, COX-2 inhibition by celecoxib treatment improves functional outcome and reduces the associated inflammation after ICH [24]. Our results suggest that hUCB-MSCs have an anti-inflammatory effect after ICH.

The early stage after ICH involves the immediate infiltration of blood components, including red blood cells, leukocytes, macrophages, and plasma proteins. Reactive microglia peak at 3 to 7 days and neutrophils peak at 3 days [25]. Therefore, management of patients with ICH is important. Moreover, hUCB-MSCs might be neuroprotective if the cells are transplanted early after insult [26]. In previous study using brain ischemia model in rats, we observed that transplantation of hUCB-MSCs 2 days after middle cerebral artery occlusion (MCAO) could reduce infract volume and improve neurological deficits. In this study, hUCB-MSCs were transplanted at 2 days after ICH.

3. Mesenchymal stem cells (MSCs) as a regulator of inflammation

The paradigm for the role of MSCs has been changed in research. The cells were used as feeder layers that provide a proper niche for culture condition and then as reparative cells that can repair of damaged tissues [27]. Recent studies demonstrate that the cells crosstalk with components of the immune system and they reveal the mechanisms of both anti- and pro-inflammatory effects [28]. In response to inflammatory molecules, MSCs secrete the immunomodulatory cytokines including, prostaglandin 2, transforming growth factor-beta 1(TGF-β1), hepatocyte growth factor (HGF), stromal cell-derived factor 1 (SDF-1), nitrous oxide, indoleamine 2,3-dioxygenase, IL-4, IL-6, IL-10, IL-1 receptor antagonist and soluble tumor necrosis factor-α receptor [29].

In this study, we obtained the cytokine array data of hUCB-MSCs from Medipost Inc. The cytokine array was performed to investigate that the paracrine effect of hUCB-MSCs on host cell leading to cartilage repair for osteoarthritis (OA) patients [30]. We identified immunomodulatory cytokines associated with neuroinflammation from the cytokine array data. There are six cytokines including, brain-derived neuroptophic factor (BDNF), ciliary neurotrophic factor (CNTF), intracellular adhesion molecule-5 (ICAM-5), interleukin-1 receptor

antagonist (IL-1 ra), macrophage colony-stimulating factor (M-CSF) and oncostatin M (OSM).

BDNF is a member of the neurotrophin growth factor family. In animal model, exogenous BDNF modulates local inflammation in ischemic brain tissues [31]. CNTF is a member of the four alpha-helical cytokine family and a neurotrophic cytokine as modulator in the inflamed nervous system [32]. ICAM-5 (telencephalin) is a member of the immunoglobulin (Ig) superfamily. ICAM-5 is involved in immune privilege of the brain [33]. IL-1 is a pro-inflammatory cytokine and a key mediator of neuronal damage after acute brain injury. IL-1Ra improves measures of brain injury by inhibiting inflammation in subarachnoid hemorrhage(SAH) animal model [34]. M-CSF is a molecule that can influence microglial phenotype. M-CSF is considered a key factor in regulating microglial inflammatory responses in the damaged brain [35]. OSM is a pleiotropic member of the IL-6 family of neuropoietic cytokines and modulates inflammatory responses [36]. These immunomodulatory foctors were up-regulated in inflammatory environment. This data suggest that the immunomodulators secreted from hUCB-MSCs may reduce inflammatory factors and, in turn, improve recovery from neurological deficit.

Recently, MSCs have been considered to have a multilateral

paracrine effects and a better therapeutic effect than a single factor. In this study, we also observed that hUCB-MSCs graft improved neurological recovery after ICH. It is likely that hUCB-MSCs secrete anti-inflammatory factors, which may modulate the inflammatory environment of ICH. Therefore, to completely understand the paracrine effects of hUCB-MSCs in ICH, it is necessary to investigate the mechanisms of the inflammatory modulators.

Ⅴ. References

1. van Asch CJ, Luitse MJ, Rinkel GJ, van der Tweel I, Algra A, et al. (2010) Incidence, case fatality, and functional outcome of intracerebral haemorrhage over time, according to age, sex, and ethnic origin: a systematic review and meta-analysis. The Lancet Neurology 9: 167-176.
2. Xi G, Keep RF, Hoff JT (2006) Mechanisms of brain injury after intracerebral haemorrhage. The Lancet Neurology 5: 53-63.
3. Morgenstern LB, Hemphill JC, Anderson C, Becker K, Broderick JP, et al. (2010) Guidelines for the Management of Spontaneous Intracerebral Hemorrhage A Guideline for Healthcare Professionals From the American Heart Association/American Stroke Association. Stroke 41: 2108-2129.
4. Gonzales NR (2013) Ongoing Clinical Trials in Intracerebral Hemorrhage. Stroke 44: S70-S73.
5. Lindvall O, Kokaia Z (2006) Stem cells for the treatment of neurological disorders. Nature 441: 1094-1096.
6. Andres RH, Guzman R, Ducray AD, Mordasini P, Gera A, et al. (2008) Cell replacement therapy for intracerebral hemorrhage. Neurosurgical focus 24: E16.
7. Dalous J, Larghero J, Baud O (2012) Transplantation of

umbilical cord-derived mesenchymal stem cells as a novel strategy to protect the central nervous system: technical aspects, preclinical studies, and clinical perspectives. Pediatric research 71: 482-490.

8. Wang S-P, Wang Z-H, Peng D-Y, Li S-M, Wang H, et al. (2012) Therapeutic effect of mesenchymal stem cells in rats with intracerebral hemorrhage: reduced apoptosis and enhanced neuroprotection. Molecular medicine reports 6: 848-854.

9. Liao W, Zhong J, Yu J, Xie J, Liu Y, et al. (2009) Therapeutic benefit of human umbilical cord derived mesenchymal stromal cells in intracerebral hemorrhage rat: implications of anti-inflammation and angiogenesis. Cellular Physiology and Biochemistry 24: 307-316.

10. Aronowski J, Zhao X (2011) Molecular pathophysiology of cerebral hemorrhage secondary brain injury. Stroke 42: 1781-1786.

11. Zhang R, Liu Y, Yan K, Chen L, Chen X-R, et al. (2013) Anti-inflammatory and immunomodulatory mechanisms of mesenchymal stem cell transplantation in experimental traumatic brain injury. Journal of neuroinflammation 10: 106.

12. Wang J, Doré S (2007) Inflammation after intracerebral hemorrhage. Journal of Cerebral Blood Flow & Metabolism

27: 894-908.

13. Keep RF, Hua Y, Xi G (2012) Intracerebral haemorrhage: mechanisms of injury and therapeutic targets. The Lancet Neurology 11: 720-731.
14. Zhou Y, Wang Y, Wang J, Anne Stetler R, Yang Q-W (2013) Inflammation in intracerebral hemorrhage: From mechanisms to clinical translation. Progress in neurobiology.
15. Lehnardt S (2010) Innate immunity and neuroinflammation in the CNS: The role of microglia in Toll-like receptor-mediated neuronal injury. Glia 58: 253-263.
16. Taylor RA, Sansing LH (2013) Microglial responses after ischemic stroke and intracerebral hemorrhage. Clinical and Developmental Immunology 2013.
17. Wang J, Rogove AD, Tsirka AE, Tsirka SE (2003) Protective role of tuftsin fragment 1-3 in an animal model of intracerebral hemorrhage. Annals of neurology 54: 655-664.
18. Wang J (2010) Preclinical and clinical research on inflammation after intracerebral hemorrhage. Progress in neurobiology 92: 463-477.
19. Sansing LH, Harris TH, Kasner SE, Hunter CA, Kariko K (2011) Neutrophil depletion diminishes monocyte infiltration and improves functional outcome after

experimental intracerebral hemorrhage. Intracerebral Hemorrhage Research: Springer. pp. 173-178.

20. Figiel I (2008) Pro-inflammatory cytokine TNF-alpha as a neuroprotective agent in the brain. Acta Neurobiol Exp (Wars) 68: 526-534.
21. Hua Y, Wu J, Keep RF, Nakamura T, Hoff JT, et al. (2006) Tumor necrosis factor-α increases in the brain after intracerebral hemorrhage and thrombin stimulation. Neurosurgery 58: 542-550.
22. Lei B, Dawson HN, Roulhac-Wilson B, Wang H, Laskowitz DT, et al. (2013) Tumor necrosis factor alpha antagonism improves neurological recovery in murine intracerebral hemorrhage. J Neuroinflammation 10: 103.
23. Minghetti L (2004) Cyclooxygenase-2 (COX-2) in inflammatory and degenerative brain diseases. Journal of Neuropathology & Experimental Neurology 63: 901-910.
24. Chu K, Jeong S-W, Jung K-H, Han S-Y, Lee S-T, et al. (2004) Celecoxib induces functional recovery after intracerebral hemorrhage with reduction of brain edema and perihematomal cell death. Journal of Cerebral Blood Flow & Metabolism 24: 926-933.
25. Ziai WC (2013) Hematology and Inflammatory Signaling of Intracerebral Hemorrhage. Stroke 44: S74-S78.

26. Qureshi AI, Mendelow AD, Hanley DF (2009) Intracerebral haemorrhage. The Lancet 373: 1632-1644.
27. Prockop DJ, Oh JY (2012) Mesenchymal stem/stromal cells (MSCs): role as guardians of inflammation. Molecular Therapy 20: 14-20.
28. Bernardo ME, Fibbe WE (2013) Mesenchymal stromal cells: sensors and switchers of inflammation. Cell stem cell 13: 392-402.
29. Murphy MB, Moncivais K, Caplan AI (2013) Mesenchymal stem cells: environmentally responsive therapeutics for regenerative medicine. Experimental & molecular medicine 45: e54.
30. Jeong SY, Kim DH, Ha J, Jin HJ, Kwon SJ, et al. (2013) Thrombospondin-2 secreted by human umbilical cord blood-derived mesenchymal stem cells promotes chondrogenic differentiation. STEM CELLS 31: 2136-2148.
31. Jiang Y, Wei N, Zhu J, Lu T, Chen Z, et al. (2011) Effects of brain-derived neurotrophic factor on local inflammation in experimental stroke of rat. Mediators of inflammation 2010.
32. Linker RA, Mäurer M, Gaupp S, Martini R, Holtmann B, et al. (2002) CNTF is a major protective factor in demyelinating CNS disease: a neurotrophic cytokine as modulator in neuroinflammation. Nature medicine 8: 620-624.

33. Tian L, Lappalainen J, Autero M, Hänninen S, Rauvala H, et al. (2008) Shedded neuronal ICAM-5 suppresses T-cell activation. Blood 111: 3615-3625.
34. Greenhalgh AD, Brough D, Robinson EM, Girard S, Rothwell NJ, et al. (2012) Interleukin-1 receptor antagonist is beneficial after subarachnoid haemorrhage in rat by blocking haem-driven inflammatory pathology. Disease models & mechanisms 5: 823-833.
35. Smith AM, Gibbons HM, Oldfield RL, Bergin PM, Mee EW, et al. (2013) M-CSF increases proliferation and phagocytosis while modulating receptor and transcription factor expression in adult human microglia. Journal of neuroinflammation 10: 85.
36. Ruprecht K, Kuhlmann T, Seif F, Hummel V, Kruse N, et al. (2001) Effects of oncostatin M on human cerebral endothelial cells and expression in inflammatory brain lesions. Journal of Neuropathology & Experimental Neurology 60: 1087-1098.

국문 초록

목적: 뇌졸중의 한 형태인 대뇌출혈은 높은 장애 발생의 위험성과 사망률을 보이는 난치병이다. 인간 제대혈 유래 중간엽 줄기세포는 대뇌출혈 이후에 오는 뇌 손상을 복원시키는 잠재적 능력을 갖고 있다. 본 연구의 목적은 대뇌출혈 쥐 모델에서 인간 제대혈 유래 중간엽 줄기세포의 이식이 유익한 효과가 있는지 알아보고, 인간 제대혈 유래 중간엽 줄기세포가 대뇌출혈 후 발생하는 이차적인 염증 반응을 감소시키는 지 알아보고자 하였다.

재료 및 방법: 콜라게네이즈 유도 대뇌출혈 쥐 모델에 인간 제대혈 유래 중간엽 줄기세포를 이식했다. 대뇌출혈 후 2, 9, 16, 30일 에, 행동학적 결과를 측정하기 위해서 회전봉 검사와 체지 배치 검사를 시행하였다. 이식 4주 후에 헤마톡실린-에오신 염색을 사용하여 대뇌뇌출혈 부피를 측정하였고, 쥐의 뇌 조직에서 신경생성, 혈관생성, 항세포사멸은 면역형광 염색으로 확인하였다. 항염증 요소들인[TNF-α, COX-2, microglia 그리고 neutrophils]은 이식 3일 후에 면역형광 염색, 역전사 중합효소연쇄반응법, 그리고 웨스턴블랏으로 분석하였다.

결과: 대뇌출혈 후 인간 제대혈 유래 중간엽 줄기세포 이식은 신경학적 이점과 출혈 부피의 감소의 효과와 연관되어 있었다.

대뇌출혈 후 30 일 째 시행한 면역화학 검사에서 인간 제대혈 유래 중간엽 줄기세포를 이식한 쥐들에서 대조군에 비하여 높은 수준의 신경세포의 재생과 신생혈관의 재생이 관찰되었고 세포사멸반응은 감소되어 관찰되었다. 대뇌출혈 후 대뇌실질에서의 염증 반응은 대조군에 비해서 인간 제대혈 유래 중간엽 줄기 세포를 처리한 쥐들에서 더 낮게 관찰되었다.

결론: 본 연구를 통하여 설치류의 대뇌출혈 뇌졸증 모델에서 인간 제대혈 유래 중간엽 줄기세포는 신경세포 및, 신생혈관의 재생을 촉진시키고 세포사멸을 감소시키며 대뇌출혈 후 발생하는 염증반응을 감소시켜 뇌졸증 후 유래되는 신경학적 장애를 개선시키는 것을 확인하였다.

주요어: 대뇌출혈, 인간 제대혈 유래 중간엽 줄기세포, 염증, 사이토카인인

학 번: 2010-20394